Letter Vol. 50, No. 2 / 15 January 2025 / *Optics Letters* 527

Optics Letters

Terahertz parametric detection using a lithium tantalate

Sota Mine,* Shiki Tanaka, Kodo Kawase, and Kosuke Murate

Department of Electronics, Nagoya University, Furocho, Nagoya, 464-8603, Japan
**mine.sota.v5@a.mail.nagoya-u.ac.jp*

Received 11 October 2024; revised 10 December 2024; accepted 15 December 2024; posted 16 December 2024; published 10 January 2025

Terahertz (THz) parametric detection is a highly sensitive method that upconverts a THz wave into a near-infrared beam for detection. Lithium niobate has primarily been used as the nonlinear optical crystal in this approach. However, the frequency band with high parametric gain is limited, leading to increasing interest in other nonlinear optical crystals. Here, we demonstrate that lithium tantalate provides high-sensitivity detection at low frequencies, achieving a maximum improvement of 15 dB over the 0.8–1.5 THz band.

https://doi.org/10.1364/OL.544632

Terahertz (THz)-waves have absorption peaks characteristic of many chemicals and a moderate transmission rate, which support both imaging [1] and nondestructive testing applications [2]. High-sensitivity THz-wave detection is therefore critical, and THz parametric detection based on stimulated polariton scattering using stimulated phonon–photon resonance has become an active area of research [3–6]. This approach enables ultra-sensitive THz-wave detection at room temperature by upconverting THz waves to more easily detectable wavelengths, such as those in the visible and near-infrared range. To expand bandwidth and enhance sensitivity in THz parametric detection, the use of an optical crystal with a high nonlinear optical coefficient, a high damage threshold, and a low absorption coefficient is essential. Lithium niobate (LN, $LiNbO_3$) meets these criteria [7–9]. However, other nonlinear optical crystals are needed for high-sensitivity detection at frequencies below 0.8 THz and above 3 THz, where the parametric gain of $LiNbO_3$ is low. Nonlinear optical crystals such as KTP [10] and DAST [11] have been used for this purpose. Lithium tantalate (LT, $LiTaO_3$) has optical properties nearly identical to those of LN [12], but LT exhibits greater parametric gain at lower frequencies because its A_1 phonon mode occurs at a lower frequency. On the other hand, because of its high absorption coefficient in the THz band, it is challenging to use it as a THz source, and its application in the THz-wave region has been limited. However, in THz detection, the impact of crystal absorption is less significant compared to its use as a THz source, making the introduction of LT into THz parametric detection a viable option. Here, we used LT to detect THz waves. Although LT generated THz waves less efficiently compared with LN, it improved THz-wave detection sensitivity in the 0.8–1.5 THz range. This frequency range is suitable for applications in nondestructive testing [2] and imaging [1], and our results will contribute to the further development of these methodologies.

During THz parametric detection, when both a THz wave and a pump beam are incident on a nonlinear optical crystal, the Stokes beam (hereafter referred to as the detection Stokes beam) corresponding to the difference frequency is generated in a direction that satisfies the non-collinear phase matching condition. A near-infrared detector can thus sensitively record THz waves at room temperature. The Stokes beam intensity changes nonlinearly with the intensity of the incident THz wave. Ultra-high-sensitive THz detection has been achieved through multi-stage amplification of the detection Stokes beam, using nonlinear optical crystals following spatial removal of parametric fluorescence noise [3] or pump beam scatter by high-performance wavelength filters [4].

LN supports THz parametric wavelength conversion due to its transparency across a broad optical region, high nonlinear optical coefficient, and high damage threshold. Here, LT, with optical properties nearly identical to those of LN, served as a nonlinear optical crystal that enhanced low-frequency THz parametric detection. The nonlinear and electro-optical coefficients of LN and LT are listed in Table 1.

The nonlinear optical coefficient indicates the conversion efficiency in optical parametric wavelength conversion using only light waves, whereas the electro-optical coefficient reflects the conversion efficiency mediated by lattice vibrations. Although the nonlinear optical constant of LT is lower than that of LN, their electro-optical coefficients are nearly identical. There are two types of parametric gain: gain associated with THz-wave amplification and gain associated with Stokes beam amplification. In THz parametric source, the parametric gain related to THz-wave amplification is critical. Conversely, in THz parametric detection, the parametric gain from Stokes beam amplification is predominant [17]. The parametric gain for THz-wave amplification is heavily influenced by the absorption coefficient of the THz wave. As a result, LT crystals demonstrate limited gain under these conditions. In contrast, the parametric gain for Stokes beam amplification is mainly determined by the nonlinear optical coefficient and the electro-optical coefficient, with minimal influence from absorption [17]. Consequently, the parametric gain of LT in THz parametric detection is comparable to that of LN.

Table 1. Nonlinear Optical and Electro-optical Coefficients of LN and LT [13–16]

	Nonlinear optical coefficient	Electro optical coefficient
LN	$d_{33} = 25.0$	$r_{33} = 30.8$
LT	$d_{33} = 14.0$	$r_{33} = 30.3$

Below, we sequentially compare the gains (experiment 1), THz-wave detection (experiment 2), and THz-wave generation (experiment 3) capabilities of LN and LT. First, the frequency dependence of the Stokes beam intensity after THz parametric amplification with LN and LT was measured, as shown in Fig. 1 (experiment 1). The pump beam from a microchip laser (Optoquest Co. Ltd., Japan) was optically amplified to 40 mJ per pulse and collimated to a beam diameter of 0.9 mm. The seed beam was amplified from 40 mW (the continuous-wave power of an external cavity diode laser) to 300 mW. MgO:LN and MgO:LT (both from Yamaju Ceramics Co., Ltd., Japan), each 50 mm in length along the x axis, were irradiated with a pump beam of 5.4 mJ/pulse (beam diameter: 1 mm along the z axis and 300 μm along the y axis) and a continuous-wave seed beam of 300 mW. The Stokes beam generated simultaneously with the THz wave was measured using an energy meter. Here, we employed a flattened pump beam to generate the Stokes beam efficiently with a small amount of pump energy [18]. Figure 2(a) shows that the maximum Stokes beam intensities of LN and LT were very similar, suggesting nearly identical parametric gains. Although the LN Stokes beam intensity peaked above 2 THz, the LT intensity peaked within the 1–2 THz range. LT thus exhibited a higher parametric gain at lower frequencies due to its A_1 phonon mode frequency of 200 cm^{-1}, which is lower than that of LN (248 cm^{-1}). However, Stokes beams remain unaffected by absorption within the crystals. In practical THz parametric detection, the THz wave is introduced from an external source to the nonlinear optical crystal, rendering the absorption coefficient in the THz frequency range a pivotal determinant of detection sensitivity. The LN and LT absorption coefficients, derived from the dielectric function, are shown in Fig. 2(b), with parameters obtained from [19] and [20]. Both absorption coefficients exponentially increase as the frequency approaches the A_1 phonon mode. Notably, LT displays a large absorption coefficient at frequencies above 2 THz, corresponding to reduced sensitivity in THz parametric detection, as expected.

Next, we measured the frequency dependence of the minimum detection energy in THz parametric detection using LN and LT, as shown in Fig. 1 (experiment 2), with an LN-based injection-seeded THz parametric generator (is-TPG) [2] serving

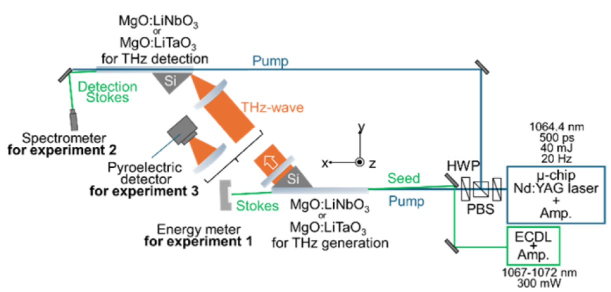

Fig. 1. Experimental setup of is-TPG and THz parametric detection using LN and LT. HWP, half-wave plate; PBS, polarized beam splitter; ECDL, external cavity diode laser.

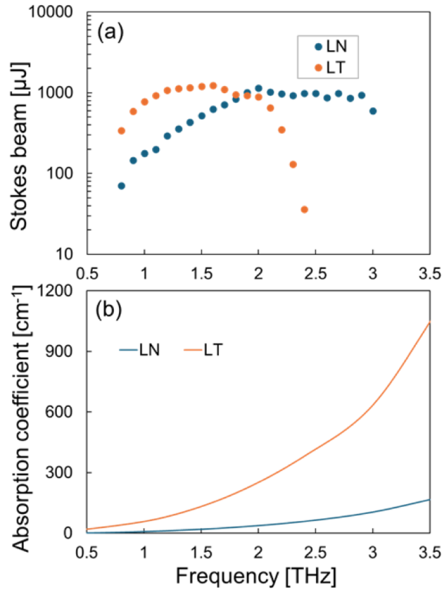

Fig. 2. Frequency dependencies of the (a) Stokes beam intensities and (b) absorption coefficients of LN and LT.

as the source. THz waves were generated with an LN-based is-TPG, and the outputs at each frequency were calibrated using a pyroelectric detector (JASCO Corporation, Japan). The nonlinear optical crystals were irradiated with pump beams of 0.7 mm in diameter, using 2.5 mJ/pulse for LN and 5 mJ/pulse for LT. These pump energies were experimentally determined to achieve the optimal detection sensitivity. For each crystal, there is an optimal pump beam energy, beyond which further increases do not improve the minimum detection energy. Excessive pump beam energy leads to increased parametric fluorescence, which causes gain competition with the detection Stokes beam. The dimensions of the LN crystal (x, y, and z) were 50, 4, and 5 mm, respectively, while those of LT were 70, 4, and 5 mm. Although the LN crystal was approximately 20 mm shorter than the LT, a 40-mm-long LN crystal is known to efficiently mediate THz parametric wavelength conversion, making this length adequate [21]. A THz wave was introduced into the LN and LT nonlinear optical crystals through an Si prism coupler, and the resulting detection Stokes beams were observed using a spectrometer (S150-I-3648; Solar Laser Systems, Harrietsham, UK) with an exposure time of 1000 ms; data from 50 THz-wave pulses were integrated. The energy of the incident THz wave was progressively attenuated using three calibrated TFA-4 THz attenuators (Microtech Instruments, Inc., Eugene, OR, USA). The minimum detection energy was determined as the point at which the signal equaled the noise level.

Figure 3 shows that the minimum energies of LN- and LT-based THz parametric detection varied by frequency. LN-based THz parametric detection (blue dots) ranged from several tens of aJ between 0.8 and 1.4 THz; sensitivity reached approximately 0.5 aJ at 1.7 THz. LT-based THz parametric detection was more sensitive overall, with minimum detection energy in the range of several aJ from 0.8 to 1.4 THz. Notably, at 0.8 THz, the minimum detection energy for LT was approximately 15 dB lower than that of LN, likely due to the high parametric gain of LT at low frequencies as shown in Fig. 2 (a). According to Fig. 2(a), the parametric gain of LT is high up to approximately 1.8 THz, and it was thought that LT would show high sensitivity up to this

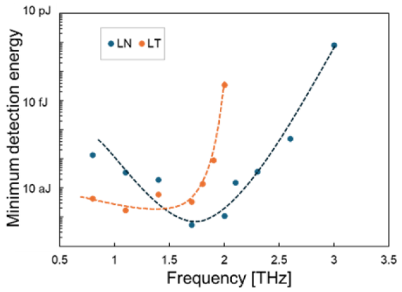

Fig. 3. Frequency dependencies of the minimum LN- and LT-based energies in THz-wave parametric detection.

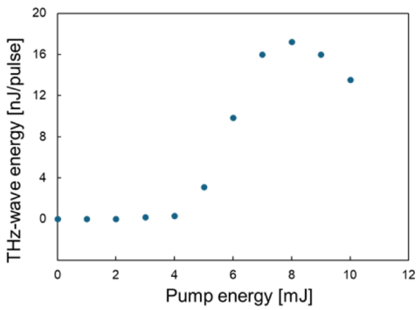

Fig. 4. Input/output characteristics of is-TPG using LN.

frequency region. However, the slight difference in the frequency characteristics of the minimum detection energy is thought to be due to the crystal absorption that occurs when THz waves enter the crystal (Fig. 2(b)). Above 1.8 THz, LT-based THz detection sensitivity declined because of high THz absorption, whereas LN sensitivity decreased above 2.5 THz.

Although sub-0.8 THz detection sensitivity could not be measured due to the limited output bandwidth of the LN-based is-TPG, sensitivity can be inferred from the frequency dependence of the Stokes beam [Fig. 2(a)]; the minimum LT detection energy was lower than that of LN, even below 0.8 THz. The low-frequency range, where LT has high sensitivity, is suitable for nondestructive testing because many reagents have fingerprint spectra and the transmittance of various shielding materials is also high [2].

Finally, we confirmed the parametric gain for THz-wave amplification by comparing the THz output when LN and LT were used for THz parametric generation, the reverse process of THz parametric detection. We constructed an is-TPG using either LN or LT, as shown in Fig. 1(experiment 3), then evaluated THz-wave source performance. The dimensions of the LN crystal (x, y, and z) were 50, 4, and 5 mm, respectively, while those of LT were 70, 4, and 5 mm. The THz waves generated by both LN and LT were coupled to free space using identically shaped Si prism couplers [22]. The frequencies of the generated THz waves were 1.1 THz; the waves were focused by a lens into a pyroelectric detector.

Figure 4 shows the input–output characteristics of the is-TPGs using LN and LT. The maximum output of the LN-based is-TPG (blue dots) was approximately 17 nJ when the pump operated at around 8 mJ. Several factors may explain the saturation observed at or above 8 mJ; here, it is likely due to variations in the location of THz-wave generation with changes in pump beam intensity, as well as alterations in the coupling efficiency of the Si prism [16]. In contrast, the LT-based is-TPG did not generate THz waves even when pumped up to 10 mJ. This result can be attributed to the strong dependence of the parametric gain in the is-TPG on the crystal absorption of THz waves, which prevents sufficient gain from being achieved with LT. Therefore, LT is suboptimal for parametric THz-wave generation.

We utilized a nonlinear LT optical crystal to improve the sensitivity of low-frequency THz parametric detection. Compared with LN, LT exhibited a lower center frequency for parametric gain and a lower minimum detection energy in the 0.8–1.5 THz band, which is commonly used for nondestructive testing and imaging. Although LT did not facilitate parametric THz generation, it provided effective THz-wave detection, suggesting that similar crystals with high nonlinear optical constants are also suitable.

Funding. Japan Society for the Promotion of Science KAKENHI (22J20963, 22H00212, 24K00943); ASPIRE Program (JPMJAP2340); Japan Science and Technology Agency (JST) FOREST Program (JPMJFR212J).

Acknowledgment. The authors would like to express their gratitude to Yamaju Ceramics Co., Ltd., for providing the LN and LT crystals used in this research.

Disclosures. The authors declare no conflicts of interest.

Data availability. Data underlying the results presented in this paper are not publicly available at this time but may be obtained from the corresponding author upon reasonable request.

REFERENCES

1. H. Minamide, K. Nawata, Y. Moriguchi, *et al.*, Rev. Sci. Instrum. **92**, 093002 (2021).
2. K. Murate, S. Mine, and K. Kawase, IEEE J. Sel. Top. Quantum Electron. **29**, 8500813 (2023).
3. H. Sakai, K. Kawase, and K. Murate, Opt. Lett. **45**, 3905 (2020).
4. T. Pfeiffer, M. Kutas, B. Haase, *et al.*, Opt. Express **28**, 29419 (2020).
5. T. Pfeiffer, J. Klier, G. von Freymann, *et al.*, Opt. Express **30**, 27572 (2022).
6. D. J. Jubgang Fandio, A. Vishnuradhan, E. K. Yalavarthi, *et al.*, Opt. Lett. **49**, 1556 (2024).
7. J. Hebling, K.-L. Yeh, M. C. Hoffmann, *et al.*, J. Opt. Soc. Am. B **25**, B6 (2008).
8. S. W. Jolly, N. H. Matlis, F. Ahr, *et al.*, Nat. Commun. **10**, 2591 (2019).
9. L. Guiramand, J. E. Nkeck, X. Ropagnol, *et al.*, Photonics Res. **10**, 340 (2022).
10. Y. Wang, C. Hu, C. Yan, *et al.*, Opt. Lett. **47**, 5853 (2022).
11. S. Fan, F. Qi, T. Notake, *et al.*, Opt. Express **23**, 7611 (2015).
12. B. Sun, X. Bai, J. Liu, *et al.*, Laser Phys. **24**, 035402 (2014).
13. R. Kremer, A. Boudrioua, P. Moretti, *et al.*, Opt. Commun. **219**, 389 (2003).
14. R. S. Weis and T. K. Gaylord, Appl. Phys. A **37**, 191 (1985).
15. J. L. Casson, K. T. Gahagan, D. A. Scrymgeour, *et al.*, J. Opt. Soc. Am. B **21**, 1948 (2004).
16. X. Xiao, S. Liang, J. Si, *et al.*, Crystals **13**, 1233 (2023).
17. K. Kawase, J.-I. Shikata, and H. Ito, J. Phys. D: Appl. Phys. **35**, R1 (2002).
18. S. Mine, M. Abe, K. Kawase, *et al.*, IEEE Trans. Terahertz Sci. Technol. **13**, 153 (2023).
19. A. Buzády, M. Unferdorben, G. Tóth, *et al.*, J. Infrared, Millimeter, Terahertz Waves **38**, 963 (2017).
20. A. S. Barker and R. Loudon, Phys. Rev. **158**, 433 (1967).
21. S. Mine, K. Kawase, and K. Murate, Opt. Lett. **47**, 1113 (2022).
22. K. Kawase, J.-I. Shikata, H. Minamide, *et al.*, Appl. Opt. **40**, 1423 (2001).